Fabrication of Metal Nanoparticles Using Toroidal Plasmid DNA as a Sacrificial Mold

Jacopo Samson,[†,∥] Alessandro Varotto,[†,∥] Patrick C. Nahirney,[§] Alfredo Toschi,[‡] Irene Piscopo,[⊥] and Charles Michael Drain[†,§,*]

[†]Department of Chemistry and Biochemistry, [‡]and the Department of Biological Sciences, Hunter College and Graduate Center of the City University of New York, 695 Park Avenue, New York, New York 10065, [§]The Rockefeller University, 1230 York Avenue, New York, New York 10065, and [⊥]EM consultant, EM CONSULTING, Huntington, New York 11743. [∥]J.S. and A.V. contributed equally to this work.

ABSTRACT A new method for synthesizing gold, nickel, and cobalt metal nanoparticles at room temperature from metal salts employing plasmid DNA in a toroidal topology as a sacrificial mold is presented. The diameter of the toroidal DNA drives the formation and size of the nanoparticle, and UV light initiates the oxidation of the DNA and concomitant reduction of the DNA bound metal ions. The nanoparticles were characterized by atomic force microscopy (AFM), transmission electron microscopy (TEM), and electron diffraction (ED).

KEYWORDS: metallic nanodisc · nanoparticles · plasmid DNA · sacrificial mold · template · torus

The fabrication of nanomaterials of metals, ceramics, inorganics, and organic dyes is widely investigated because these materials possess unusual or unexpected properties that can be exploited for a wide range of applications.[1−4] There are diverse methods of fabricating metal nanoparticles including reduction of the metal salts with reducing agents,[5] pyrolysis,[6−8] laser ablation,[9,10] and photoreduction.[11,12] The average nanoparticle size ranges from a few nanometers to over 100 nm. The size, shape, and dispersity depend on the synthetic methods and can be controlled by adjusting thermodynamic as well as kinetic parameters.[6]

A variety of templates can be employed in the preparation of nanoparticles to control the size and spatial distribution. Nanostructured materials such as carbon nanotubes,[13] aggregates,[14] organic polymers, biopolymers,[15−17] and biological systems such as viruses[18] can be used as a platform on which nanoparticles can be adsorbed or synthesized as a means to order the nanoparticles in two or three dimensions. Nanoparticles can be formed and stabilized in a variety of matrixes such as gels,[19,20] polymers,[21] and biopolymers,[22] which can also induce specific shapes. Nanoparticles can be formed inside self-organized biomimetic rings that control the growth of the nanoparticle, but these rings are formed in low yields.[23] For molding nanomaterials in nanocavities or templates, the ideal mold can be made in high yields, is monodispersed, and is topologically well defined.

A plasmid is a circular extrachromosomal DNA molecule capable of replicating autonomously in bacterial hosts[24] and can be made in large quantities using standard molecular biology procedures.[25] Besides being monodispersed biopolymers, plasmid DNA adopts a variety of topologies such as relaxed, linear supercoiled, and toroidal depending on environmental conditions such as temperature, pH, and ionic strength. A recent report demonstrated that ionic strength can maximize the toroidal topology of plasmid DNA.[26] Also, the toroid thickness is a salt-dependent phenomenon that can be controlled with the ionic strength and that a given plasmid will always form the same size toroids under the same conditions.[26] In general, the size of the toroid depends on the number of base pairs, the sequence of the plasmid, and environmental factors. As a proof-of-principle, we present herein the use of the toroidal form of pcDNA 3.1(+) plasmid DNA (Figure 1) as a monodispersed biopolymer nanocavity mold for the formation of disc-shaped nanoparticles of several types of metals.

In addition to being monodispersed and easy to synthesize in high yields, this approach exploits several properties of plasmid DNA: (1) DNA is well-known to bind cations at the negatively charged phosphate backbone with various affinities,[27] (2) metal ion binding favors formation of

*Address correspondence to cdrain@hunter.cuny.edu.

Received for review November 11, 2008 and accepted January 16, 2009.

Published online January 30, 2009.
10.1021/nn800758n CCC: $40.75

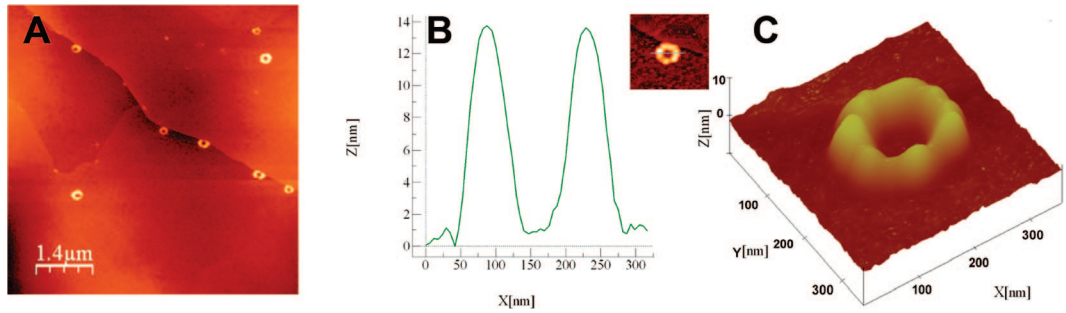

Figure 1. (A) AFM height image of the toroidal topology of plasmid pcDNA 3.1(+) on a HOPG substrate. (B) Height analysis of inset (top right corner). (C) 3-Dimensional AFM image of the plasmid shown in B.

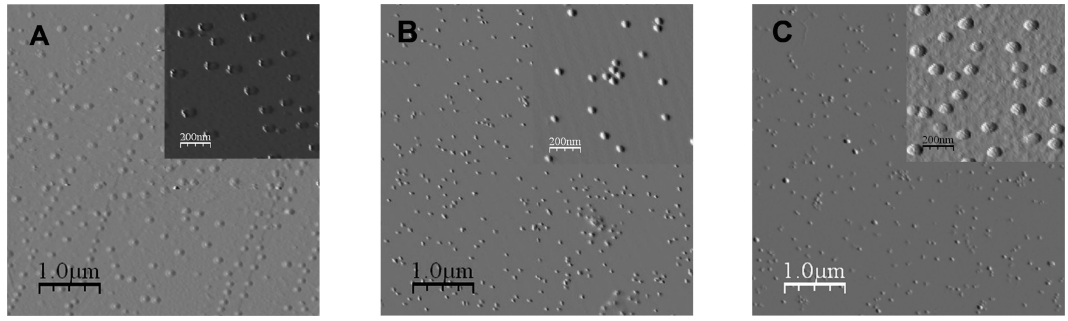

Figure 2. AFM amplitude images of metal nanoparticles obtained from photo-initiated reduction of metal ions bound to plasmid pcDNA 3.1(+) sacrificial mold: (A) gold; (B) nickel; (C) cobalt particles.

toroidal plasmid DNA structures,[26] (3) the size of plasmid, therefore the size of the toroid, is easy to vary,[18,19] (4) DNA has a well-established UV light initiated oxidation chemistry.[28−30]

RESULTS AND DISCUSSION

Fabrication of Nanoparticles. Incubation of low concentrations of Me_3PAuCl, $NiCl_2 \cdot (H_2O)_6$, or $CoCl_2 \cdot (H_2O)_6$ with pcDNA 3.1(+) plasmid DNA, which has 5428 base pairs, does not affect the distribution of the three main topologies significantly (Supporting Information, Figure S5). UV irradiation (254 nm) of the plasmid shows a redistribution of the conformations and degradation in the presence of the three metal ions. Photo-oxidation and degradation of the DNA mold upon exposure of the sample to 254 nm UV light results in reduction of the metal ions such that the plasmid DNA acts as a sacrificial mold and drives the formation of the nanoparticles.

After incubation of the plasmid DNA suspension (10 μL of a 1 μg/μL original solution) with the gold, nickel, or cobalt salts (12 mM) overnight in the dark at 4 °C, the nanoparticles were prepared by irradiating the solution for one hour with UV light (λ = 254, 10 μW/cm^2 using a UVGL-25 compact UV lamp by UVP). The solutions were then cast onto AFM or TEM substrates through a 0.2 μm syringe filter. (See Supporting Information, Figure S7, for controls without the plasmid.)

Characterization of the Nanoparticles. The sizes of the nanoparticles were characterized with both AFM (Figure 2) and TEM (Figure 3) to get accurate measurements of the heights and widths of the metal nanoparticles, respectively. The histograms of the AFM-measured heights and the TEM-measured horizontal dimensions are presented in Chart 1. The vertical and horizontal dimensions of the metal nanoparticles reveal that these nanoparticles are disc-shaped. The average height of the nickel and cobalt nanodiscs obtained from pcDNA 3.1(+) templates is 13 ± 2 nm, while for gold the average height is 8 ± 2 nm. These nanoparticle heights correspond with the 12−14 nm vertical dimension of the plasmid. The 40−60 diameters of the metallic nanodiscs correspond to the inner diameter of the toroidal plasmid (Figure 1), and the differences are discussed below.

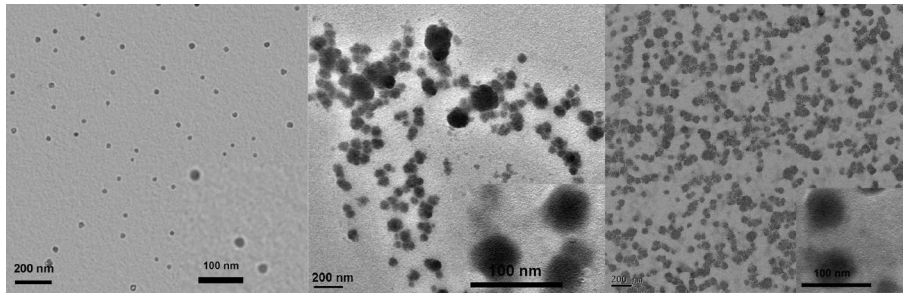

Figure 3. TEM images were used to assay the diameters of metal nanodiscs obtained from photo-initiated reduction of metal ions bound to plasmid pcDNA 3.1(+) sacrificial mold: (A) gold nanoparticles, (B) nickel nanoparticles, and (C) cobalt nanoparticles.

The small differences in the nanoparticle heights and widths for the three metals can be attributed to several factors. As mentioned before,

the relative distribution of the toroidal/supercoiled condensation state *versus* the linear and relaxed forms does not significantly change upon binding of low concentrations of these metals (Supporting Information, Figure S5) and is in agreement with a previous study.[26] However, the dimensions of the toroidal condensation state of the plasmid are sensitive to the binding of the different metal ions,[31−33] and the morphology of the plasmid changes during the formation of the nanoparticles as it is degraded under UV irradiation. Photoinduced metal coating of linear DNA with concomitant photo-oxidation of DNA to yield nanowires has been reported.[34,35] In our study, even though the mechanism of photoreduction of the metal may occur in a similar fashion, the circular morphology of the toroidal DNA clearly drives the formation of nanodisc topologies. The size of the nanodisc is correlated to the inner diameter of the plasmid and circular DNA but is not exactly the same. When the plasmid is incubated with the gold salt or nickel salt and irradiated for 5−20 min with the UV light, there is a significant contraction in the plasmid height (Supporting Information, Figure S3). After UV irradiating for 20 min, the forming particle is still surrounded by filaments of DNA (Supporting Information, Figure S12). To probe the possible mechanism(s) for the formation of nanoparticles, we used AFM scans of a drop of solution containing pcDNA and $NiCl_2$ on HOPG after UV irradiation for 20, 40, and 60 min. The images suggest that there is a contraction of the plasmid soon after irradiation. After 20 and 40 min, filaments of DNA are still visible, whereas after 60 min the photodegradation process is complete, and only nanoparticles are visible (Supporting Information, Figure S11).

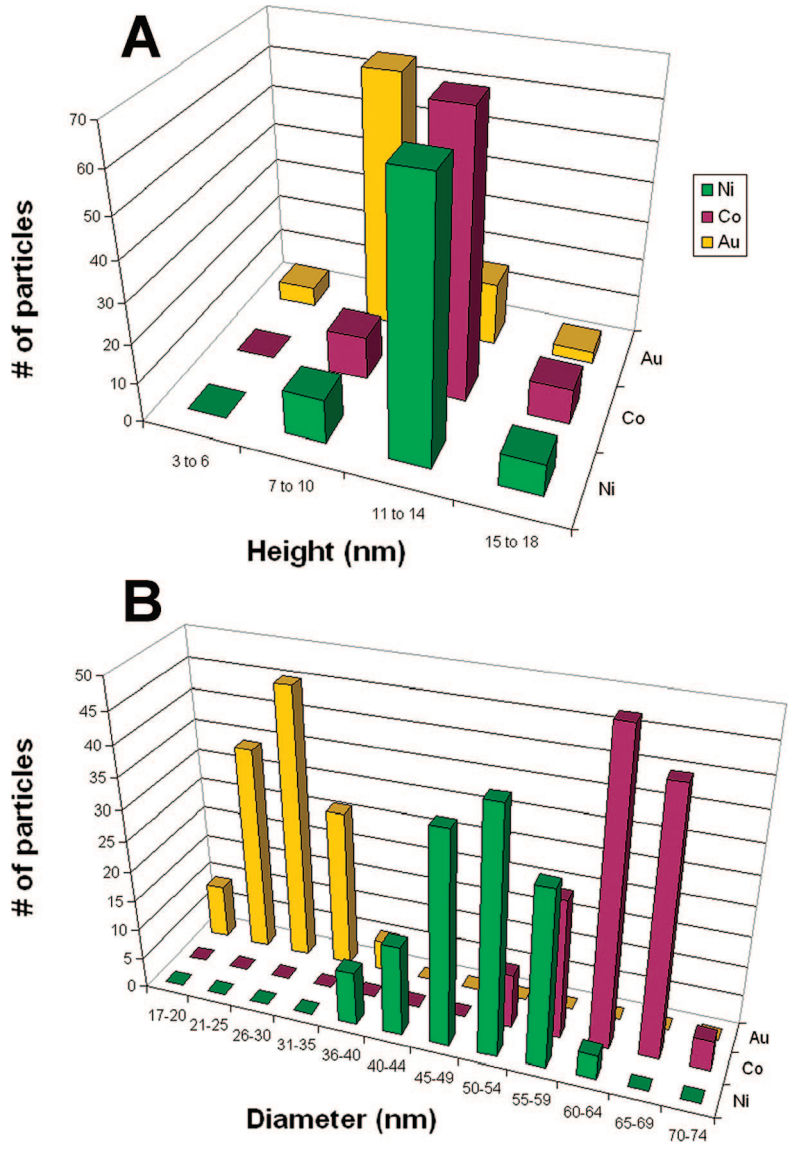

Chart 1. (A) Histograms of the height distribution determined by AFM and (B) histograms of the diameter distribution determined by TEM: nickel (green), cobalt (purple), and gold (yellow) nanoparticles obtained using a pcDNA 3.1(+) template.

Electron diffraction analysis (Figure 4) suggests that most of the nanodiscs are composed only of the metal atoms. Some DNA fragments adsorbed to the outside of the nanoparticle are occasionally observed in both AFM and TEM images. As noted above, incomplete degradation of the plasmid DNA and DNA decorated with small metal nanoparticles are observed in experiments

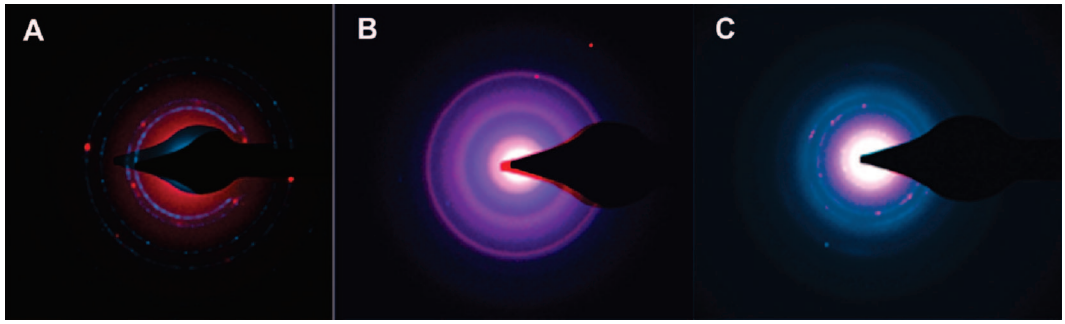

Figure 4. ED patterns in red of the prepared nanodiscs of (A) gold, (B) nickel, and (C) cobalt. The corresponding standards are superimposed and are in blue.

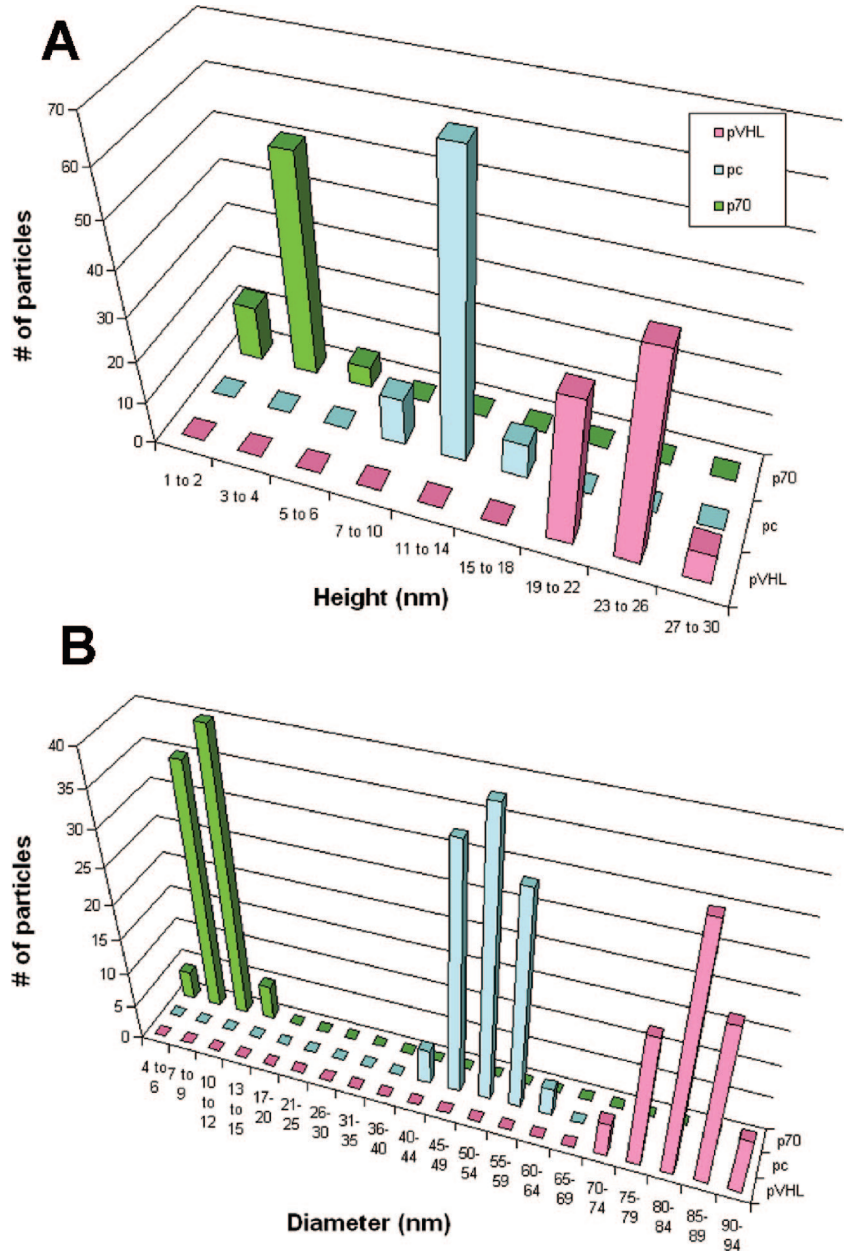

Chart 2. (A) Histograms of the height and (B) histogram of the diameter distribution determined by AFM of nickel nanoparticles using p70 (olive green), pcDNA (light blue), and pVHL (pink) as molds. The diameter measurements were estimated from the AFM height images; a 10 nm ultra-sharp tip was utilized to minimize the error due to the tip convolution effect.

with shorter UV irradiation times. Only amorphous clusters of various sizes are observed in control experiments with no plasmid DNA. Chemical reduction of these metal ions with hydrazine anhydrous results in similar nanodiscs with similar shapes, but the plasmid DNA surrounds the nanoparticles or is entrained in the nanoparticles depending on growth conditions (Supporting Information, Figure S11,12). Taken together, these data suggest that small changes in the toroid dimensions of the plasmid DNA can be induced by the binding of different metal ions[19−22] and that the detailed mechanism and kinetics of nanodisc formation may be somewhat metal ion dependent. As with other template methods,[23] it is likely that the increased concentration of the metal ion inside the toroid relative to the outside drives the formation of the nanodiscs. In the case of a sacrificial mold, the competing rates of nanoparticle formation *versus* mold degradation, which also may be metal ion dependent, will also influence the size and morphology of the products.

Use of Different Plasmids. Other plasmids with different numbers of base pairs and sequences can adopt similar structures but with different sizes, though the size of the toroidal condensation state does not linearly scale with the number of base pairs. The plasmid pRc/CMV-(HA)-pVHL, abbreviated as pVHL, has *ca.* 8000 bp and also adopts toroidal conformations (Supporting Information, Figure S9). The same procedures as above using the larger pVHL plasmid result in larger gold, nickel, and cobalt nanodiscs with different heights (Supporting Information, Figure S2). A much smaller circular DNA containing 70 base pairs is able to mold the formation of 3 $\pm$ 0.5 nm high by 13 $\pm$ 5 nm wide nanoparticles of nickel (Supporting Information, Figure S10). Note that the AFM error for these smallest nanoparticles is greater due to convolution with the 10 nm tip curvature so that the actual diameter is less than observed. Chart 2 shows the histogram of the height as well as the diameter distribution of nanoparticles using the two different plasmids and p70.

CONCLUSIONS

In conclusion, we have synthesized narrowly dispersed nanodiscs at room temperature using UV light and a biological sacrificial toroidal plasmid DNA mold. Toroidal plasmids are readily available in large quantities, easy to purify, rigid, and monodispersed. The size of the particles is dictated by the topology of the template, metal ion binding, and the mechanism of formation. The method is quite general and may be applicable to DNA/RNA structures with more complex topologies. Future studies will investigate the formation of other types of nanoparticle; e.g., this work suggests that it may be possible to form nanorings by controlling the synthetic conditions. The method uses materials and equipment found in most undergraduate teaching laboratories.

EXPERIMENTAL SECTION

Materials. Me_3PAuCl and $Co(II)Cl_2 \cdot 6H_2O$ were purchased from Sigma Aldrich, and $Ni(II)Cl_2 \cdot 6H_2O$ was purchased from Fisher Scientific. The pcDNA3.1(+) plasmid was obtained from Invitrogen. The 12 mM stock solutions of metal chlorides were prepared in nanopure water. The gold solution was prepared by adding an equal portion of deionized water to 100 mL of a 24 mM stock solution of Me_3PAuCl dissolved in acetone.

Instrumentation. Atomic Force Microscopy (AFM) was conducted utilizing a Veeco Multimode SPM. All the images were acquired in tapping mode using a rectangular cantilever from Mikromasch NSC15 series AlBS (nominal radius of curvature, RC = 10 nm, 325 kHz, and a spring constant = 40 N/m); its backside is aluminum-coated. The Veeco SPM is equipped with software for processing the data which has been used together with Nanotech WSxM 4.0 Develop 12.[36] While the height measurements are accurate and reproducible from AFM experiments, the effect of the tip convolution (10 nm RC) is known to alter the lateral dimensions of the objects scanned.[37]

Transmission electron microscopy (TEM) was performed using carbon-coated copper grids (EMS). The samples were imaged at 80 and 120 kV using a Tecnai G2 Biotwin (FEI). ED patterns were collected at 120 kV. The TEM images have been processed using Image J.

Synthesis of the Nanoparticles. Three 1 mL Eppendorf tubes containing 10 μL of a suspension of plasmid pcDNA 3.1(+) (5428 base pairs, stored in TE buffer at −20 °C, concentration: 1 μg/μL) were incubated overnight at 4 °C in the dark after adding 50 μL of a 12 mM solution of Me_3PAuCl, $Ni(II)Cl_2$, or $Co(II)Cl_2$, respectively, with a final salt concentration of 10 mM. The solutions were then irradiated by UV light for a total of 60 min (λ = 254 nm, 10 μW/cm^2 using a UVGL-25 compact UV lamp by UVP). The solutions were finally filtered through a 0.2 μm syringe filter (Nalgene).

The samples for AFM experiments were prepared by slow evaporation of 5 μL of solution on mica or highly ordered pyrolytic graphite (HOPG, SPI supplies). Images were collected from several different batches, and the distribution of diameters and heights was averaged between them. Samples for TEM were prepared similarly on the carbon-coated copper grids. We have observed that TEM analysis can transform metal salts deposited on the TEM grid into metallic materials.

The standard reduction potentials (at 25 °C) of the three metal ions used are: + 1.69 V for $Au_{(s)}$ (from $Au^{1+}{}_{(aq)} + 1e^{-1}$), −0.25 V for $Ni_{(s)}$ (from $Ni^{2+}{}_{(aq)} + 2e^{-1}$), and −0.28V for $Co_{(s)}$ ($Co^{2+}{}_{(aq)} + 2e^{-1}$).[38]

Acknowledgment. This work was supported by the NSF (CHE-0554703) to C.M.D. Hunter College science infrastructure is supported by the National Science Foundation, the National Institutes of Health including the RCMI program (G12-RR-03037), and the City University of New York. The Rockefeller University EM laboratory is also acknowledged. pRc/CMV-(HA)-pVHL was a generous gift of Dr. Michael Ohh (University of Toronto, Toronto, ON, Canada), and the 70 bp circular DNA was a generous gift of Dr. Smita Patel (University of Medicine and Dentistry of New Jersey, Piscataway, New Jersey).

Supporting Information Available: Control preparation, pcDNA3.1(+) data, pVHL data, experimental, AFM data, gel electrophoresis, and particle size histograms. Further data and discussion on the mechanism of nanoparticle formation. This material is available free of charge *via* the Internet at http://pubs.acs.org.

REFERENCES AND NOTES

1. Lu, A.-H.; Salabas, E. L.; Schüth, F. Magnetic Nanoparticles: Synthesis, Protection, Functionalization, and Application. *Angew. Chem., Int. Ed.* **2007**, *46*, 1222–1244.
2. Feldheim, D. L.; Foss, C. A., Jr. *Metal Nanoparticles: Synthesis, Characterization, and Applications*; Marcel Dekker, Inc.: New York and Basel, 2002.
3. Drain, C. M.; Smeureanu, G.; Patel, S.; Gong, X.; Garno, J.; Arijeloye, J. Porphyrin Nanoparticles as Supramolecular Systems. *New J. Chem.* **2006**, *30*, 1834–1843.
4. Frenkel, J.; Doefman, J. Spontaneous and Induced Magnetization in Ferromagnetic Bodies. *Nature* **2003**, *126*, 274–275.
5. Guo, F.; Zheng, H.; Yang, Z.; Qian, Y. Synthesis of Cobalt Nanoparticles in Ethanol Hydrazine Alkaline System (EHAS) at Room Temperature. *Mater. Lett.* **2002**, *56*, 906–909.
6. Puntes, V. F.; Krishnan, K.; Alivisatos, A. P. Synthesis of Colloidal Cobalt Nanoparticles with Controlled Size and Shapes. *Top. Catal.* **2002**, *19*, 145–148.
7. Puntes, V. F.; Krishnan, K. M.; Alivisatos, A. P. Synthesis, Self-Assembly, and Magnetic Behavior of a Two-Dimensional Superlattice of Single-Crystal ε-Co Nanoparticles. *Appl. Phys. Lett.* **2001**, *78*, 2187–2189.
8. Kim, S. W.; Park, J.; Jang, Y.; Chung, Y.; Hwang, S.; Hyeon, T.; Kim, Y. W. Synthesis of Monodisperse Palladium Nanoparticles. *Nano Lett.* **2003**, *3*, 1289–1291.
9. Takami, A.; Kurita, H.; Koda, S. Laser-Induced Size Reduction of Noble Metal Particles. *J. Phys. Chem. B* **1999**, *103*, 1226–1232.
10. Kazakevich, P. V.; Simakin, A. V.; Voronov, V. V.; Shafeev, G. A. Laser Induced Synthesis of Nanoparticles in Liquids. *Appl. Surf. Sci.* **2006**, *252*, 4373–4380.
11. Vesperinas, A.; Eastoe, J.; Jackson, S.; Wyatt, P. Light-Induced Flocculation of Gold Nanoparticles. *Chem. Commun.* **2007**, 3912–3914.
12. Fang, Q.; He, G.; Cai, W. P.; Zhang, J.-Y.; Boyd, I. W. Palladium Nanoparticles on Silicon by Photo-Reduction Using 172 nm Excimer UV Lamps. *Appl. Surf. Sci.* **2004**, *226*, 7–11.
13. Chen, P.; Wu, X.; Lin, J.; Tan, K. L. Synthesis of Cu Nanoparticles and Microsized Fibers by Using Carbon Nanotubes as a Template. *J. Phys. Chem. B* **1999**, *103*, 4559–4561.
14. Banerjee, I. A.; Yu, L.; Matsui, H. Cu Nanocrystal Growth on Peptide Nanotubes by Biomineralization: Size Control of Cu Nanocrystals by Tuning Peptide Conformation. *Proc. Natl. Acad. Sci. U.S.A.* **2003**, *100*, 14678–14682.
15. Sun, L.; Wei, G.; Song, Y.; Liu, Z.; Wang, L.; Li, Z. Fabrication of Silver Nanoparticles Ring Templated by Plasmid DNA. *Appl. Surf. Sci.* **2006**, *252*, 4969–4974.
16. Aldaye, F. A.; Palmer, A. L.; Sleiman, H. F. Assembling Materials with DNA as the Guide. *Science* **2008**, *321*, 1795–1799.
17. Coffer, J. L.; Bigham, S. R.; Li, X.; Pinizzotto, R. F.; Rho, Y. G.; Pirtle, R. M.; Pirtle, I. L. Dictation of the Shape of Mesoscale Semiconductor Nanoparticle Assemblies by Plasmid DNA. *Appl. Phys. Lett.* **1996**, *69*, 3851–3853.
18. Flynn, C. E.; Lee, S.-W.; Peelle, B. R.; Belcher, A. N. Viruses as Vehicles for Growth, Organization and Assembly of Materials. *Acta Materialia* **2003**, *51*, 5867–5880.
19. Maruszewski, K.; Jasiorski, M.; Hreniak, D.; Strk, W.; Hermanowicz, K.; Heiman, K. Raman Spectra of Molecules Adsorbed on Ag Centers in Sol-Gel Matrices. *J. Sol-Gel Sci. Technol.* **2003**, *26*, 83–88.
20. Antonietti, M.; Ozin, G. A. Promises and Problems of Mesoscale Materials Chemistry or Why Meso? *Chem.—Eur. J.* **2004**, *10*, 28–41.
21. Zhong, Z.; Sim, D.; Teo, J.; Luo, J.; Zhang, H.; Gedanken, A. D-Glucose-Derived Polymer Intermediates as Templates for the Synthesis of Ultrastable and Redispersible Gold Colliods. *Langmuir* **2008**, *24*, 4655–4660.
22. Ganesan, R.; Gedanken, A. Synthesis of WO3 Nanoparticles Using a Biopolymer as a Template for Electrocatalytic Hydrogen Evolution. *Nanotechnology* **2008**, *19*, 025702.
23. Djalali, R.; Samson, J.; Matsui, H. Doughnut-Shaped Peptide Nano-Assemblies and Their Applications as Nanoreactors. *J. Am. Chem. Soc.* **2004**, *126*, 7935–7939.
24. Lipps, G. *Plasmids: Current Research and Future Trends*; Caister Academic Press: Norfolk, U.K., 2008.
25. QIAGEN. QIAGEN PlasmidAmp Kit-For direct amplification of plasmid DNA from bacterial colonies, www1.qiagen.com.
26. Conwell, C. C.; Vilfan, I. D.; Hud, N. V. Controlling the Size of Nanoscale Toroidal DNA Condensates with Static

Curvature and Ionic Strength. *Proc. Natl. Acad. Sci. U.S.A.* **2003**, *100*, 9296–9301.
27. Bloomfield, V. A. Condensation of DNA by Multivalent Cations: Considerations on Mechanism. *Biopolymers* **2005**, *31*, 1471–1481.
28. Bartolini, W. P.; Johnston, M. V. Characterizing DNA Photo-Oxidation Reactions by High-Resolution Mass Measurements with Matrix-Assisted Laser Desorption/Ionization Time-of-Flight Mass Spectrometry. *J. Mass Spectrom.* **2000**, *35*, 408–416.
29. Boerner, L. J.; Zaleski, J. M. Metal Complex-DNA Interactions: From Transcription Inhibition to Photoactivated Cleavage. *Curr. Opin. Chem. Biol.* **2005**, 135–144.
30. Sinha, R. P.; Häder, D.-P. UV-Induced DNA Damage and Repair: A Review. *Photochem. Photobiol. Sci.* **2002**, *1*, 225–236.
31. Schnell, J. R.; Berman, J.; Bloomfield, V. A. Insertion of Telomere Repeat Sequence Decreases Plasmid DNA Condensation by Cobalt (III) Hexaammine. *Biophys. J.* **1998**, *74*, 1484–1491.
32. Davey, C. A.; Richmond, T. J. DNA-Dependent Divalent Cation Binding in the Nucleosome Core Particle. *Proc. Natl. Acad. Sci. U.S.A.* **2002**, *99*, 11169–11174.
33. Liu, C.; Wang, M.; Zhang, T.; Sun, H. DNA Hydrolysis Promoted by Di- and Multi-Nuclear Metal Complexes. *Coord. Chem. Rev.* **2004**, *248*, 147–168.
34. Berti, L.; Alessandrini, A.; Facci, P. DNA-Templated Photoinduced Silver Deposition. *J. Am. Chem. Soc.* **2005**, *127*, 11216–11217.
35. Burley, G. A.; Gierlich, J.; Mofid, M. R.; Nir, H.; Tal, S.; Eichen, Y.; Carell, T. Directed DNA Metallization. *J. Am. Chem. Soc.* **2006**, *128*, 1398–1399.
36. Horcas, I.; Fernández, R.; Gómez-Rodriguez, J. M.; Colchero, J. WSXM: A Software for Scanning Probe Microscopy and a Tool for Nanotechnology. *Rev. Sci. Instrum.* **2007**, *78*, 013705.
37. Wong, C.; West, P. E.; Olson, K. S.; Mecartney, M. L.; Starostina, N. Tip Dilation and AFM Capabilities in the Characterization of Nanoparticles. *J. Met.* **2007**, *59*, 12–16.
38. web.archive.org/web/20070518092613/http://www.north-land.cc.mn.us/Chemistry/standard_reduction_potentials.htm. Standard reduction potentials.